

High-efficiency silicon-compatible photodetectors based on Ge quantum dots

S. Cosentino,¹ Pei Liu,¹ Son T. Le,¹ S. Lee,¹ D. Paine,¹ A. Zaslavsky,¹ D. Pacifici,^{1,a)} S. Mirabella,² M. Miritello,² I. Crupi,² and A. Terrasi²

¹School of Engineering, Brown University, Providence, Rhode Island 02912, USA

²MATIS-IMM-CNR and Dipartimento di Fisica ed Astronomia, Università di Catania, Catania I-95123, Italy

(Received 19 January 2011; accepted 9 May 2011; published online 3 June 2011)

We report on high responsivity, broadband metal/insulator/semiconductor photodetectors with amorphous Ge quantum dots (a-Ge QDs) as the active absorbers embedded in a silicon dioxide matrix. Spectral responsivities between 1–4 A/W are achieved in the 500–900 nm wavelength range with internal quantum efficiencies (IQEs) as high as $\sim 700\%$. We investigate the role of a-Ge QDs in the photocurrent generation and explain the high IQE as a result of transport mechanisms via photoexcited QDs. These results suggest that a-Ge QDs are promising for high-performance integrated optoelectronic devices that are fully compatible with silicon technology in terms of fabrication and thermal budget. © 2011 American Institute of Physics. [doi:10.1063/1.3597360]

Group IV semiconductor quantum dots (QDs) have attracted much attention in applied research for their interesting optoelectronic properties¹ and for their potential compatibility with very large scale integration technology. Recently, Si and Ge QDs have stimulated increased interest as viable materials for high responsivity photodetectors (PDs) in the visible and near infrared wavelength ranges. For example, Si QD PDs have been shown to achieve peak responsivities in the range of 0.4–2.8 A/W, and optoelectronic conversion efficiencies as high as 200%.^{2,3} Compared to Si QDs, SiO₂-encapsulated Ge QDs are characterized by lower synthesis temperatures,^{4,5} as well as higher absorption coefficients due to localized states at the Ge/SiO₂ interface.^{6–8} However, so far the maximum responsivity reported for Ge QD PDs has been 0.13 A/W at $\lambda=820$ nm (Ref. 9) and 1.8 A/W at $\lambda=600$ nm,¹⁰ with the latter devices produced via a high-temperature anneal at 900 °C.

In this letter we report on photocurrent measurements of metal-insulator-semiconductor (MIS) PD with high density a-Ge QDs embedded in the SiO₂ layer. Our Ge-rich SiO₂ films of ~ 230 nm thickness were fabricated by rf-magnetron cosputtering deposition of a SiO₂ and a Ge target onto a (100) *n*-Si substrate ($\sim 8 \times 10^{18}$ cm⁻³ doping) maintained at 400 °C.⁸ Transmission electron microscope (TEM) micrographs show the presence of small, densely and homogeneously distributed a-Ge QDs in the as-grown film with mean QD size of 3 nm.⁸ The top contact of the MIS structure was fabricated by sputter-depositing a fully transparent 55 nm thick indium-zinc-oxide (IZO) film of 2×10^{-4} Ω cm resistivity, whereas the bottom contact was made to the *n*-Si substrate using silver paste. The insets of Fig. 1 show a schematic of the device structure, as well as a TEM image of the a-Ge QDs, and a schematic band diagram in reverse bias, indicating both optical absorption and carrier transport.

Figure 1 shows a comparison of the current-voltage $I(V)$ curves in the dark and under white light illumination, with

the *n*-Si substrate grounded and the top contact swept from -10 to 10 V in 10 mV steps. In the dark, the $I(V)$ is strongly rectifying with $\sim 10^4$ rectification ratio at ± 4 V. Similar $I(V)$ characteristics were reported previously in Si (Ref. 11) and Ge (Refs. 6 and 12) QD-containing MIS structures and attributed to hopping conduction through the QDs in the barrier. Within this framework, the large current in forward bias is carried by electrons tunneling from the electron accumulation layer in the *n*-Si substrate (where their density increases rapidly with V and reduces the effective tunneling barrier). Instead, the low current in reverse bias is due to electrons tunneling from the IZO through a barrier that is relatively insensitive to V . Upon white light illumination, the forward bias $I(V)$ remains largely unaffected, but there is a strong increase in the reverse current by a factor of $>10^2$, similar to the results reported by Shieh *et al.*² in a Si QD-containing MIS structure.

Figure 2(a) shows $I(V)$ measurements by illuminating the device at various incident λ in the 400–1100 nm range under continuous wave illumination. A clear dependence on

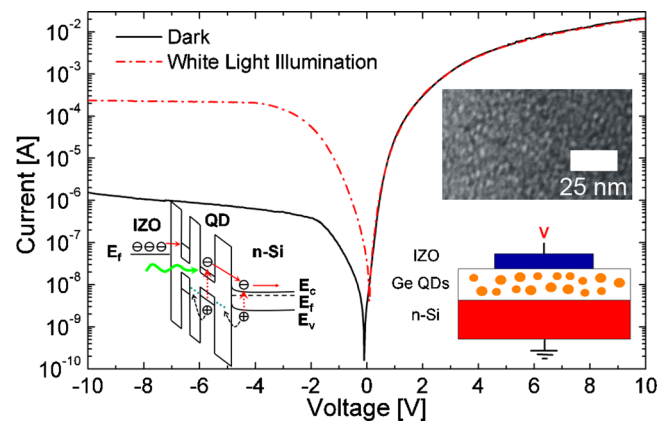


FIG. 1. (Color online) Current-voltage $I(V)$ characteristics in dark and under white light illumination of MIS PD with Ge QDs embedded in a silicon dioxide layer. The insets show a transmission electron micrograph of the as-deposited Ge QDs (courtesy: G. Nicotra, see Ref. 8), a schematic cross-section of the device and energy band diagram in reverse bias.

^{a)}Author to whom correspondence should be addressed. Electronic mail: domenico_pacifici@brown.edu.

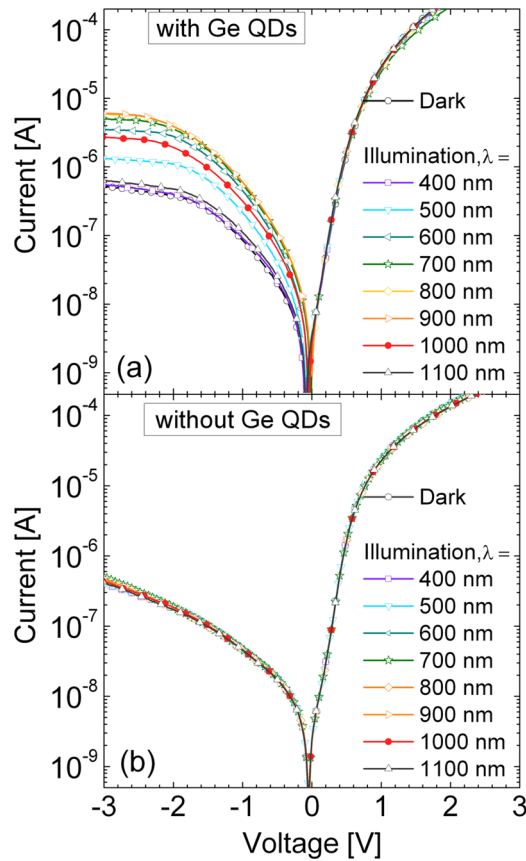


FIG. 2. (Color online) MIS PD $I(V)$ characteristics as a function of excitation wavelength λ in the 400–1100 nm range for a device with (a) and without (b) a-Ge QDs.

λ in the 500–1000 nm range is observed. Control devices with the same thickness of SiO_2 without a-Ge QDs exhibit no response for any λ [see Fig. 2(b)], indicating the key role of the Ge QDs.

Figure 3(a) shows the responsivity of a device containing a-Ge QDs as a function of λ , obtained by measuring the photogenerated current from Fig. 2(a) (defined as the difference between the total current under illumination minus the dark current at a given reverse bias) and normalizing it to the incident optical power. The responsivity at $\lambda \sim 900$ nm reaches 4 A/W at -10 V bias and ~ 1.75 A/W at a lower -2 V bias. These responsivity values are higher than results reported for MIS PDs employing Si (Ref. 2) or Ge (Refs. 9 and 13) QDs, and higher than commercial Si PDs and NREL calibrated silicon reference cell [shown in Fig. 3(a) for comparison].

Actually, spectral responsivity can be affected by the light reflected from the sample, not contributing to the photocurrent, hindering a direct correlation with the physical mechanisms underlying the photogeneration of carriers. The internal quantum efficiency (IQE) of our device can be calculated by measuring the reflectance R at normal incidence, shown in Fig. 3(b), and then normalizing the number of photogenerated carriers by the number of absorbed photons, i.e., by $(1-R)$ times the number of incident photons, for any given λ . The results are summarized in Fig. 3(c), which shows IQE as high as 700% at -10 V and $\lambda \sim 700$ nm, corresponding to a large photoconductive gain (the highest previously reported IQE for MIS PDs was $\sim 400\%$ in Ref. 10). Our IQE are higher than yet consistent with those re-

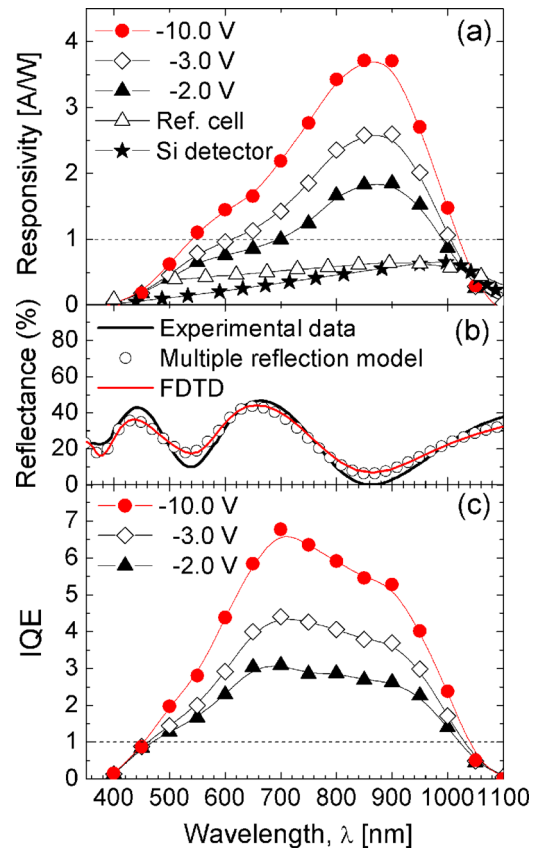


FIG. 3. (Color online) (a) Spectral responsivity of our MIS PD versus reverse bias; stars and open triangles indicate, respectively, the responsivity of a commercial Si PD and of an NREL calibrated silicon reference cell. (b) Measured reflectance spectra and simulations using a multiple reflection model and FDTD analysis. (c) IQE.

ported by Shieh *et al.*² (IQE=200%) and by Tzeng *et al.*¹⁰ (IQE=400%) for similar MIS PDs incorporating, respectively, Si or Ge QDs.

Since V drops over the thick insulating layer and since we observe gain at V as low as -2 V, we can rule out impact ionization in the Ge QDs or in the substrate as the dominant mechanism. Instead, a possible explanation for the high photoconductive gain of our PDs is as follows: (1) electron-hole pairs are photogenerated both in the a-Ge QDs and in the substrate; (2) due to the large difference in the tunneling mass, the holes are exponentially slower than electrons to tunnel between QDs in the SiO_2 ; therefore (3) a net positive (hole) charge accumulates in the a-Ge QD layer and, to maintain charge neutrality, (4) additional electrons need to be supplied from the IZO reservoir, which tunnel through the SiO_2 and contribute to the observed photocurrent. A similar gain mechanism was suggested previously for photoconductive gain in QD-containing MIS structures (where holes are trapped by Ge QDs),⁹ as well as GaN/AlGaIn metal-semiconductor-metal PDs (where holes are trapped by line defects in GaN).¹⁴

The PD responsivity depends on the electromagnetic wave distribution within the multilayered MIS structure. In order to characterize the optical properties of our device, we first fit the experimental reflectance spectra for devices with and without IZO layer, by using a multiple reflection model [Fig. 3(b)]. The fitting procedure allowed us to confirm the IZO and insulating layer thicknesses (55 nm and 230 nm, respectively) as well as determine the refractive index for the

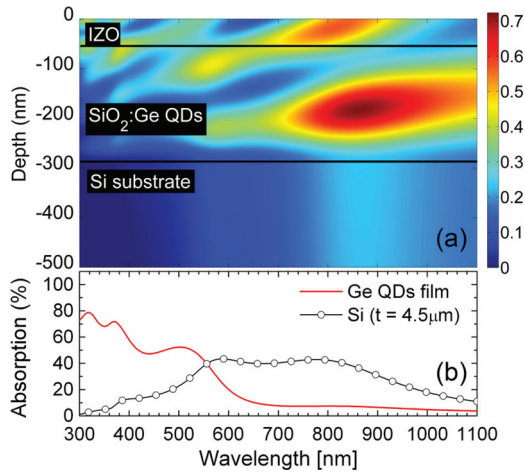


FIG. 4. (Color) (a) FDTD calculations of the electric field intensity distribution vs wavelength (300–1100 nm) and depth, normalized by the field intensity of the incident wave. (b) Fraction of incident light intensity absorbed by the Ge QDs (red line) and by the first 4.5 μm of silicon substrate (corresponding to the minority hole diffusion length).

transparent IZO (using a Cauchy model) and volume fraction of a-Ge QDs in the film ($\sim 36\%$, using the Maxwell–Garnett approximation, in good agreement with independent estimates using x-ray photoemission spectroscopy).¹⁵

We then performed finite-difference-time-domain (FDTD) calculations using a commercial software package (LUMERICAL) to reproduce the reflectance measurements [Fig. 3(b)] and calculate the electric field intensity distribution inside the PD structure, as shown in Fig. 4(a), as a function of λ and depth. At 900 nm, the electric field intensity (normalized to the incident field intensity) peaks inside the insulating layer containing the Ge QDs, although there is also leakage of incident radiation into the Si substrate. From the simulations and definition of the Poynting vector, we can estimate the fraction of absorbed light intensity occurring within the Ge QDs and the silicon substrate, respectively, as shown in Fig. 4(b). The results show that while shorter wavelengths are absorbed mostly in the Ge QDs, longer wavelengths are preferentially absorbed in the bulk Si. However, only the photogenerated holes that are created within a minority carrier diffusion length of the interface ($\sim 4.5 \mu\text{m}$ for our *n*-Si substrate) can tunnel into the Ge QDs, where they are trapped and induce the electron flow, leading to the observed photocurrent. These results demonstrate that light absorption by Ge QDs [which have an optical band gap of 1.6

eV (Ref. 8)] and in the silicon substrate is crucial for achieving a broad spectral response. Further studies are necessary to clarify the details of the photoconductive gain mechanisms and transport via photoexcited Ge QDs.

In conclusion, we have demonstrated MIS PDs containing a-Ge QDs in the SiO_2 insulator that operate in the visible and near-infrared with high IQE (up to $\sim 700\%$) and responsivity up to 4 A/W. These devices can be operated at a reverse bias as low as 2 V and can be fabricated with processing steps below 400 $^\circ\text{C}$. We attribute their high efficiency to photoconductive gain provided by the trapping of holes in the Ge QDs. These findings open a route toward the realization of high-efficiency PDs based on Ge QDs that can be easily integrated into a standard silicon complementary metal-oxide semiconductor process.

This work was performed in part at the Brown Microelectronics Facility, a member of the Materials Research Facilities Network, funded by the National Science Foundation (Grant No. DMR-0520651), and in part at the Università di Catania. The work at Brown University was in part funded by U.S. Department of Energy grant (Grant No. DE-SC0001556) and by NSF (Grant No. DMR-0804915).

¹L. Pavesi, L. Dal Negro, C. Mazzoleni, G. Franzò, and F. Priolo, *Nature (London)* **408**, 440 (2000).

²J. M. Shieh, Y. F. Lai, W. X. Ni, H. C. Kuo, C. Y. Fang, J. Y. Huang, and C. L. Pan, *Appl. Phys. Lett.* **90**, 051105 (2007).

³J. M. Shieh, W. C. Yu, J. Y. Huang, C. K. Wang, B. T. Dai, H. Y. Jhan, C. W. Hsu, H. C. Kuo, F. L. Yang, and C. L. Pan, *Appl. Phys. Lett.* **94**, 241108 (2009).

⁴B. Zhang, S. Shrestha, M. A. Green, and G. Conibeer, *Appl. Phys. Lett.* **96**, 261901 (2010).

⁵D. Pacifici, E. C. Moreira, G. Franzò, V. Martorino, F. Priolo, and F. Iacona, *Phys. Rev. B* **65**, 144109 (2002).

⁶M. Fujii, O. Mamezaki, S. Hayashi, and K. Yamamoto, *J. Appl. Phys.* **83**, 1507 (1998).

⁷Y. Maeda, *Phys. Rev. B* **51**, 1658 (1995).

⁸S. Cosentino, S. Mirabella, M. Miritello, G. Nicotra, R. Lo Savio, F. Simone, C. Spinella, and A. Terrasi, *Nanoscale Res. Lett.* **6**, 135 (2011).

⁹B. C. Hsu, S. T. Chang, T. C. Chen, P. S. Kuo, P. S. Chen, Z. Pei, and C. W. Liu, *IEEE Electron Device Lett.* **24**, 318 (2003).

¹⁰S. S. Tzeng and P. W. Li, *Nanotechnology* **19**, 235203 (2008).

¹¹M. A. Rafiq, Y. Tsuchiya, H. Mizuta, S. Oda, S. Uno, Z. A. K. Durrani, and W. I. Milne, *J. Appl. Phys.* **100**, 014303 (2006).

¹²J.-Y. Zhang, Y.-H. Ye, and X.-L. Tan, *Appl. Phys. Lett.* **74**, 2459 (1999).

¹³S. S. Tseng, I. H. Chen, and P. W. Li, *Appl. Phys. Lett.* **93**, 191112 (2008).

¹⁴S. K. Zhang, W. B. Wang, F. Yun, L. He, H. Morkoç, X. Zhou, M. Tamargo, and R. R. Alfano, *Appl. Phys. Lett.* **81**, 4862 (2002).

¹⁵See supplementary material at <http://dx.doi.org/10.1063/1.3597360> for additional information on data analysis.